Applied Computer Science 2026, vol. 22, no. 3, pp. 121–147
https://doi.org/10.35784/acs_9376

Submitted: 2026-03-18 | Revised: 2026-06-16 | Accepted: 2026-07-13

CC-BY 4.0

Keywords: adaptive particle swarm optimisation, variable-length feature selection, gene expression data, microarray data, cancer classification

Siti RAMADHANI [1,2], *Muhammad FIKRY* [1,2], *Haldi BUDIMAN* [3], *Theam Foo NG* [4], *Sumayyah DZULKIFLY* [1], *Roziana ARIFFIN* [5], *Shir Li WANG* [1*]

[1] Universiti Pendidikan Sultan Idris, Malaysia, p20221001662@siswa.upsi.edu.my, p20241001106@siswa.upsi.edu.my, sumayyah.dzul@meta.upsi.edu.my, shirli_wang@meta.upsi.edu.my
[2] Universiti Islam Negeri Sultan Syarif Kasim, Indonesia, siti.ramadhani@uin-suska.ac.id, Muhammad.fikry@uin-suska.ac.id
[3] Universitas Islam Kalimantan Muhammad Arsyad Al-Banjar, Indonesia, haldibudiman@uniska-bjm.ac
[4] Universiti Sains Malaysia, Malaysia, tfng@usm.my
[5] Premier Integrated Lab IHH, roziana.ariffin@gmail.com
[*] Corresponding author: shirli_wang@meta.upsi.edu.my

A hybrid parameter-tuning for adaptive variable-length particle swarm optimisation in cancer feature selection

Abstract

High-dimensional gene expression data pose substantial challenges for cancer classification due to extreme dimensionality, feature redundancy, and limited sample availability. Conventional Variable-Length PSO with Local Search (VLPSO-LS) relies on static acceleration coefficients and predefined inertia-weight schedules, which may limit adaptive search behaviour and increase the risk of premature convergence. To address these limitations, this study proposes a novel Variable-Length Adaptive Particle Swarm Optimisation with Local Search (VL-APSO-LS) framework. The proposed method incorporates a dynamic particle representation, adaptive inertia weight and acceleration control, and a comprehensive velocity update mechanism to enhance diversification and exploitation within a variable-length optimisation structure. The framework was evaluated on five benchmark microarray datasets (Leukaemia, SRBCT, Colon, Lymphoma, and Lung cancer) using four widely adopted classifiers. Experimental results demonstrate that VL-APSO-LS consistently improves predictive performance and feature-selection efficiency relative to VLPSO-LS and other PSO-based variants. The strong-balance performance configuration (Scheme 2) achieves an average classification accuracy of 94.39%, outperforming the baseline of 92.64%. Furthermore, it achieves the highest Accuracy-to-Feature Ratio (0.3775 vs 0.3369), indicating a superior balance between accuracy and feature compactness. Notably, the proposed method achieves perfect classification accuracy (100%) on the Leukaemia dataset and reduces the selected features in the Colon dataset to only 86, compared with over 700 features in competing approaches. Statistical validation confirms consistent non-inferiority and frequent superiority across dataset-classifier combinations, particularly when integrated with Support Vector Machine (SVM). Overall, VL-APSO-LS provides a robust, adaptive, and statistically validated optimisation framework for high-dimensional biomedical classification.

1. INTRODUCTION

Microarray technology has been widely used to analyse gene expression profiles for various diseases and medical treatments. In this context, the classification process typically requires selecting a small subset of informative genes from extremely high-dimensional datasets. The selected genes are then used to build classification models based on their expression patterns. However, gene expression datasets present several challenges, including high dimensionality, limited sample sizes, non-random noise variations, background differences among samples, feature redundancy, and nonlinear relationships among genes. Feature selection (FS) techniques play a crucial role in addressing these challenges. By identifying the most relevant genes, FS methods reduce dataset complexity, improve classification accuracy, and enhance the interpretability of predictive models (Mohamed et al., 2024). In recent years, the concept of dynamic variable-length particle representation has inspired the development of Variable-Length Particle Swarm Optimisation with Local

Search activation (VLPSO-LS) for feature selection in machine learning within the framework of population-based optimisation. This approach allows flexible solution representation by enabling particles to dynamically adjust their lengths during the optimisation process. As a result, VLPSO-LS can achieve improved optimisation performance while reducing computational costs in classification tasks (Tran et al., 2019).

Despite these advantages, the original VLPSO-LS framework does not explicitly distinguish between training and testing datasets during the optimisation process. This limitation leaves a gap in understanding how the optimisation behaviour affects model generalisation performance. In practical machine learning applications, generalisation capability and performance consistency are critical factors for evaluating model effectiveness, particularly when models are applied to unseen data in real-world scenarios (Zhang et al., 2020). To address these issues, this study proposes an improved optimisation framework. The main contributions of this study are summarised as follows:

1. Enhanced feature selection: Adaptive parameter configurations of the VLPSO algorithm, specifically for the inertia weight (w) and acceleration coefficients (c), are introduced to improve feature selection across multiple cancer datasets, including colon, small round blue cell tumour (SRBCT), lymphoma, leukaemia, and lung cancer.
2. Improved generalisation and stability: The proposed Variable-Length Adaptive Particle Swarm Optimisation with Local Search (VL-APSO-LS) demonstrates that adaptive parameter configurations for both w and c coefficients can reduce overfitting and stabilise model performance across different datasets.
3. Comprehensive classification evaluation: The selected features are evaluated using four widely used machine learning classifiers: k-nearest neighbour (KNN), decision tree (DT), Naive Bayes (NB), and Support Vector Machine (SVM) classifiers.

The remainder of this study is organised as follows. Section 2 reviews the related literature, Section 3 describes the proposed methodology, Section 4 presents the experimental results and performance evaluation, and Section 5 concludes the study.

2. PARTICLE SWARM OPTIMISATION (PSO)

PSO is one of the most well-regarded evolutionary, swarm-based algorithms in the literature and is widely employed as a feature selection algorithm for GEP, in which specific generated solutions randomly move within the search and work to obtain optimal solutions (Mohammed & Beitollahi, 2022; Shami et al., 2022). Since its initial development by Kennedy and Eberhart, numerous variants of PSO have been proposed to enhance solution quality and optimisation efficiency (Kennedy, 1997; Kennedy & Eberhart, 1997).

2.1. Fundamentals of PSO

The fundamental concept of PSO involves learning from neighbours' experiences through the communication of global best (*gbest*) information and integration of the individual's own experience (*pbest*)(Tran et al., 2016). Through iterative updates, particles adjust their positions in the search space to locate better solutions. Although the original PSO has demonstrated satisfactory optimisation performance, its learning mechanism may lead to premature convergence. This issue can limit the algorithm's ability to explore the search space effectively, especially in high-dimensional optimisation problems such as gene expression feature selection (Zhang & Sanderson, 2007; Trelea, 2003).

Traditional PSO also typically uses fixed-length particle representations, in which each particle represents a solution with a fixed number of dimensions. In high-dimensional datasets, such as microarray gene expression data, this representation may lead to large search spaces and increased computational costs, potentially resulting in suboptimal feature subset selection and reduced classification accuracy. Researchers have therefore proposed various PSO variants to improve the efficiency and robustness of optimisation. Previous studies have shown that effective parameter adjustment can significantly enhance PSO's ability to escape local optima and achieve more stable convergence toward global solutions (Jain et al., 2022).

2.2. Velocity update mechanism

In PSO, the velocity update consists of three main components: the inertia weight (w), which controls the balance between exploration and exploitation; the cognitive component (c_1), which represents a particle's

tendency to return to its own best-known position; and the social component (c_2), which represents the influence of the swarm's global best position. The inertia weight controls the balance between exploration and exploitation during the search process. The cognitive component represents a particle's tendency to return to its own best-known position (pbest), while the social component represents the influence of the swarm's global best position (gbest).

Improper parameter settings of w, c_1, and c_2 can significantly affect the algorithm's optimisation performance (Gad, 2022; Papazoglou & Biskas, 2023). If these parameters are not properly configured, the algorithm may converge prematurely or fail to explore promising regions of the search space. One of the earliest improvements to the original PSO was the introduction of the inertia weight parameter into the velocity update equation. Based on how the inertia weight is determined, these strategies can be classified into three categories: constant inertia weight, time-varying inertia weight, and adaptive inertia weight. In constant inertia weight strategies, w remains fixed throughout the optimisation process or is randomly selected within a predefined range, typically between 0.2 and 1.0. Several PSO variants, such as PSO-LSRG, BBPSO, and VNDPSO, adopt parameter settings of $c_1 = c_2 = 2.0$, with w decreasing linearly from 0.9 to 0.4.

In time-varying inertia weight strategies, w is defined as a function of time and gradually adjusted during the search process. Although these approaches dynamically change w, they are not considered fully adaptive because they do not account for the swarm's real-time state. Typically, w is initialised with a larger value to encourage exploration and gradually reduced to promote exploitation. For instance, the MFTIWPSO algorithm adopts a time-varying inertia weight within the range [1.0, 0.5] (M. Li et al., 2019). Similarly, the linearly decreasing inertia weight PSO (PSO-LDIW) used ranges such as [0.9, 0.4] or [1.2, 0.9], while random inertia weight PSO (PSO-RIW) adopted randomly generated values within the interval [1.0, 0.5] (Cao et al., 2023). Variable-Length PSO (VLPSO), which forms the baseline method in this study, employs c = 1.49445 and uses a time-varying inertia weight that decreases linearly within the range [0.9, 0.2].

The third category consists of adaptive inertia weight strategies, which dynamically adjust w based on feedback from the swarm's current state. For example, chaotic inertia weight PSO (PSO-CIW) determines w based on personal and global best positions (Ajibade et al., 2023). Other adaptive variants, such as the nonlinear inertia weight (PSO-NLIW) and an improved binary particle swarm optimisation (IBPSO), adapt both c and w parameters during the optimisation process to enhance the algorithm's global search capability (Azar et al., 2023; Ji et al., 2020; Nouri-Moghaddam, 2023). Because VLPSO currently relies on a time-varying inertia-weight mechanism, integrating adaptive parameter control is a promising direction for improving optimisation performance. Although adaptive PSO variants have demonstrated improved search capability, feature selection for high-dimensional microarray datasets is not limited to PSO-based optimisation. Various filters, embedded, wrapper, and multi-objective approaches have also been widely investigated in the literature.

Beyond PSO-based approaches, numerous feature selection methods have been successfully applied to high-dimensional microarray datasets. Filter-based techniques such as Minimum Redundancy Maximum Relevance (mRMR), Information Gain (IG), and Relief are widely used due to their computational efficiency and ability to reduce dimensionality prior to classification (Alomari et al., 2020). Embedded approaches, including Least Absolute Shrinkage and Selection Operator (LASSO), perform feature selection during model training and have demonstrated effectiveness in identifying discriminative biomarkers (Algamal et al., 2018). Wrapper-based methods such as Recursive Feature Elimination (RFE) and Genetic Algorithms (GA) have also been extensively explored to improve classification performance through iterative feature subset optimisation (Hamed et al., 2018; Peng et al., 2021). More recently, multi-objective optimisation techniques have gained attention by simultaneously considering classification accuracy and feature subset compactness. Although these methods have shown promising results, challenges remain in balancing optimisation efficiency, feature subset quality, and robustness in extremely high-dimensional gene expression datasets. Consequently, adaptive PSO-based optimisation remains a promising research direction, particularly for high-dimensional feature selection problems that require efficient exploration of large search spaces.

Despite the success of these approaches, PSO-based optimisation remains attractive because of its strong global search capability and flexibility in exploring large combinatorial feature spaces. Nevertheless, conventional PSO still faces several limitations when applied to high-dimensional feature selection problems, particularly in terms of representation scalability and computational efficiency. These limitations motivated the development of variable-length optimisation strategies such as VLPSO.

2.3. Limitations of conventional PSO

Despite PSO's effectiveness, several limitations arise when applying the algorithm to high-dimensional feature selection problems. One key challenge is the reliance on fixed-length particle representations, which require substantial memory and increase computational time when handling high-dimensional datasets such as gene expression profiles (Saraf et al., 2023).

To address this limitation, Variable-Length optimisation strategies have been proposed. In the Variable-Length PSO (VLPSO) framework, particles can dynamically change their dimensionality during the optimisation process, allowing more flexible representation of candidate solutions. The length of each particle in this method is dynamically adjusted by either truncating or appending dimensions to the particle representation, while preserving learned information in the retained dimensions.

The VLPSO approach enables the algorithm to maintain diversity while adapting its search-space representation to the evolving optimisation landscape. For example, in a swarm divided into five divisions, the initial particle lengths may be set to 1000, 2000, 3000, 4000, and 5000 dimensions, respectively (Tran et al., 2019). If the third division achieves the highest average fitness, its particle length becomes the new reference length for the swarm, and the particle lengths of other divisions are proportionally adjusted as shown in Figure 1. This proportional resizing helps preserve meaningful feature information while removing redundant dimensions that do not contribute to optimisation performance. As a result, the algorithm can improve search efficiency and accelerate convergence toward more discriminative feature subsets (Bi et al., 2023; Shami et al., 2025).

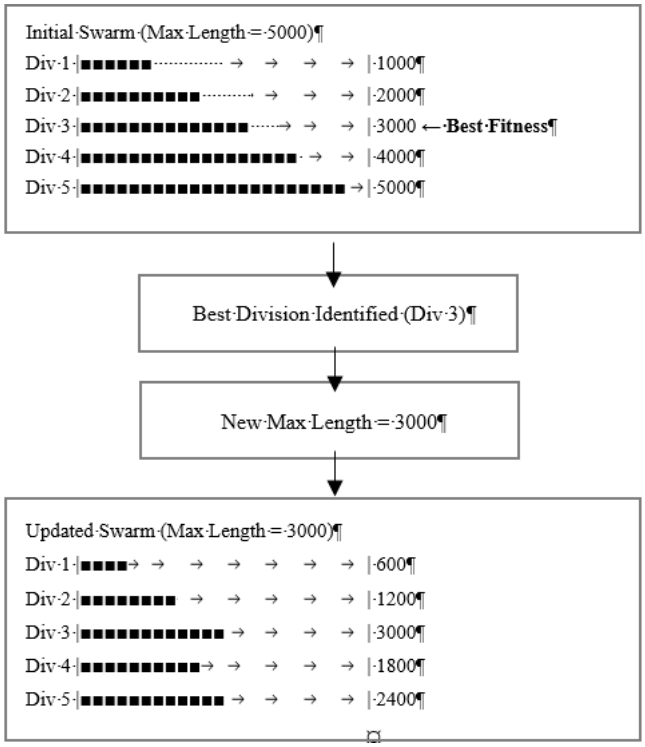


Fig. 1. Example of length changing in a swarm with five divisions

However, many existing studies have not clearly separated the treatment of training and testing data when evaluating variable-length optimisation approaches, leaving a gap in understanding their generalisation behaviour. Furthermore, evaluating optimisation algorithms solely by training performance may lead to misleading conclusions due to overfitting. Therefore, classification performance must also be assessed using unseen testing data. In this study, model performance is evaluated using k-fold cross-validation to ensure reliable generalisation performance across both training and testing datasets (Ampomah et al., 2020; Camalan et al., 2021).

To rigorously evaluate the proposed optimisation framework, statistical testing methods are employed. Traditional null-hypothesis significance testing methods, such as the paired t-test, have limitations when dealing with small sample sizes (Wasserstein & Lazar, 2016). Therefore, this study complements traditional

statistical analysis with non-inferiority testing, which determines whether the proposed method performs no worse than a baseline method beyond a predefined margin (Ravenzwaaij et al., 2019; Stefanos et al., 2020). In this research, non-inferiority analysis is applied to classification accuracy across cancer datasets using a non-inferiority margin of $\delta = 1$ percentage point and a one-sided significance level of $\alpha = 0.05$. The proposed VL-APSO-LS method is compared with the baseline VLPSO-LS using both the Wilcoxon signed-rank test and a non-inferiority framework to ensure a robust, statistically meaningful evaluation, and is also compared with the PSO state of the art.

3. PROPOSED APPROACH

Feature selection and classifier design play a critical role in high-dimensional microarray-based cancer classification, where extreme dimensionality and limited sample sizes often degrade predictive performance. To address these challenges, this study proposes an enhanced Variable-Length Adaptive Particle Swarm Optimisation with Local Search (VL-APSO-LS) framework designed to improve convergence stability and feature compactness.

3.1. Framework overview

The experimental framework is designed to systematically evaluate the proposed optimisation strategy through controlled baseline comparison, multi-classifier validation, rigorous statistical testing, and benchmarking against state-of-the-art methods. The results demonstrate that the adaptive variable-length mechanism improves convergence stability and feature compactness while maintaining statistically validated performance gains. The overall experimental architecture is illustrated in Figure 2.

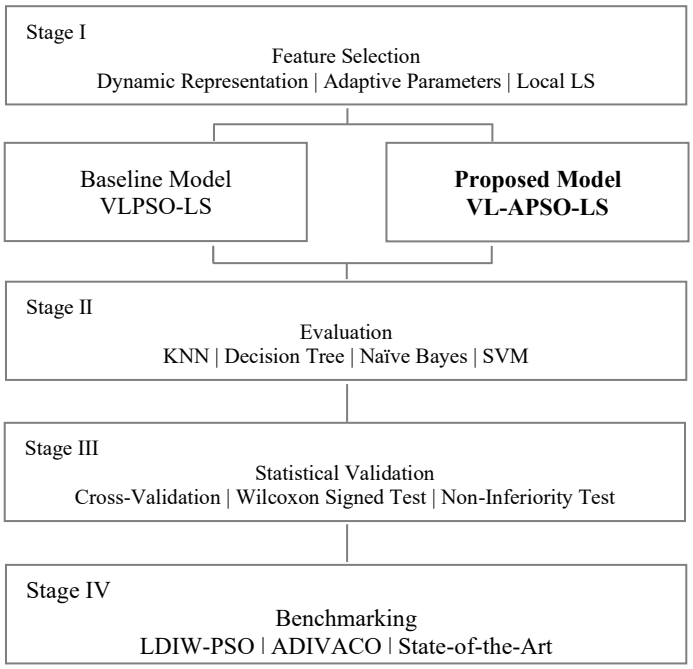


Fig. 2. Experimental framework

The framework in Figure 2 is organised into four sequential stages to ensure methodological transparency and rigorous evaluation. Stage I focuses on feature selection, where the baseline VLPSO-LS and the proposed VL-APSO-LS are executed in parallel under identical conditions. This controlled configuration enables a direct assessment of the impact of adaptive parameter learning and dynamic representation on convergence behaviour and feature compactness. Stage II evaluates the discriminative capability of the selected feature subsets using multiple classifiers. By incorporating K-Nearest Neighbour (KNN), Decision Tree (DT), Naïve Bayes (NB), and Support Vector Machine (SVM), the framework mitigates classifier-specific bias and provides a

comprehensive evaluation of generalisation performance. Stage III introduces statistical validation through cross-validation, Wilcoxon signed-rank testing, and non-inferiority analysis to determine whether observed performance improvements are statistically reliable rather than attributable to random variation. Finally, Stage IV extends the analysis to benchmarking against established state-of-the-art optimisation strategies, including Linear Descending Inertia Weight (LDIW-PSO) and Adaptive Dynamic Inertia Weight and Acceleration Coefficient Optimisation (ADIVACO). This final stage ensures that the proposed framework is evaluated not only against its baseline but also within the broader optimisation landscape.

3.2. Comparative PSO-based algorithms

Previous enhancements to PSO, LDIW-PSO, and ADIVACO have demonstrated improved balance between exploration and exploitation. LDIW-PSO is a widely used PSO variant designed to improve the balance between exploration and exploitation during the optimisation process. In this method, the inertia weight *w* decreases linearly over iterations, allowing the swarm to perform global exploration in the early stages and gradually shift toward local exploitation in later stages. The inertia weight is calculated as:

$$w^{(k)} = \left(\frac{(w_{max}-w_{min})\times(Max_k-k)}{(Max_k)} + w_{min}\right) \times z^k \tag{1}$$

Where *w* denotes the inertia weight, z^k is a chaotic mapping μ from the previous iteration, with the formula of logistic mapping is

$$z^k = \mu \times z^{k-1} \times (1-z) \tag{2}$$

The acceleration coefficients of LDIW-PSO is expressed as

$$c = \left(\frac{(c_{max} - c_{min}) \times (Max_k - k)}{(Max_k)} + w_{min}\right) \times c_{min} \tag{3}$$

Where c_{max} and c_{min} is the range of c. This mechanism improves convergence speed and helps guide particles toward promising regions of the search space. However, LDIW-PSO may still suffer from premature convergence when dealing with highly multimodal optimisation problems.

ADIVACO is an enhanced PSO variant that introduces adaptive control mechanisms for both the inertia weight and acceleration coefficients. Unlike standard PSO or LDIW-PSO, which use adaptive or time-varying parameters, ADIVACO dynamically adjusts these parameters based on the optimisation state to improve the exploration-exploitation balance. The adaptive inertia weight is computed using a hyperbolic tangent formulation:

$$w = \mu \tanh \delta \tag{4}$$

Where μ is a scaling parameter, and δ represents the time-varying control variable. The acceleration coefficients of ADIVACO is expressed as

$$c_1 = c_2 = \mu \cosh \psi \tag{5}$$

Where $c_1 = c_2$ represent the cognitive and social acceleration coefficients, respectively.

Both LDIW-PSO and ADIVACO employ the conventional PSO velocity update mechanism and maintain a fixed particle length during the optimisation process. These algorithms are commonly evaluated using benchmark optimisation functions and have not yet been extensively tested on real-world optimisation problems.

3.3. Datasets description

The microarray medical datasets used in this study are publicly available online (Zhu et al., 2007). Table 1 shows the breakdown of the total number of samples used for classification across various cancer datasets. For each dataset, the total number of samples, the number of training and testing samples, and the number of original features prior to any feature selection are reported.

Tab. 1. Summary of dataset characteristics

Dataset	Leukaemia	SRBCT	Colon	Lymphoma	Lung Cancer
Class	2	4	2	3	2
Total Samples	72	83	62	62	181
Original Feature	7129	2308	2000	4026	12533

- Leukaemia: Leukaemia is broadly classified into Acute Myeloid Leukaemia (AML) and Acute Lymphoblastic Leukaemia (AML). This dataset contains 72 samples, including 47 'ALL' and 25 AML samples, with 7,129 gene expression features.
- Small Round Blue Cell Tumour (SRBCT): The dataset consists of four classes: neuroblastoma (arising in tissues along the spine, chest, abdomen, or pelvis), rhabdomyosarcoma (originating from muscle tissue), Ewing's sarcoma (affecting soft tissue around bones), and Wilms tumour (a form of kidney cancer). The dataset includes a relatively balanced number of training and testing samples (63 and 20, respectively), with a high-dimensional feature space of 2,308 features.
- Colon Tumour: The dataset includes 62 samples obtained from colon tumour patients, consisting of 40 tumour biopsies (negative, *-ve*) and 22 normal healthy biopsies (positive, *+ve*) collected from the same individuals. The original dataset contains 6,500 gene expression features, of which 2,000 were selected for analysis.
- Lymphoma: It is a cancer of the lymphatic system, including the lymph nodes and the spleen, and is commonly categorised into Hodgkin and non-Hodgkin lymphoma. The lymphoma dataset exhibits a sample distribution similar to that of the SRBCT dataset but contains slightly more features, for a total of 4,026.
- Lung cancer: It originates in lung tissue. The lung cancer dataset has the largest number of samples among the datasets considered, with 181 samples in total, of which 103 are used for testing. This dataset also has the highest feature dimensionality, comprising 12,533 gene expression features.

The use of multiple benchmark datasets is essential to evaluate the robustness and generalisation capability of the proposed VL-APSO-LS framework. The selected datasets differ substantially in terms of dimensionality, sample size, class distribution, and biological characteristics. Evaluating the proposed method across diverse datasets allows the experiment to assess whether the adaptive optimisation mechanism consistently improves feature selection performance across different problem complexities and to avoid dataset-specific conclusions.

3.4. Adaptive variable-length PSO for FS

The proposed VL-APSO-LS extends the conventional variable-length particle swarm optimisation framework by incorporating adaptive parameter control within the velocity update mechanism. In the standard VLPSO-LS, particles dynamically adjust their representation length to determine the number of selected features; however, the search behaviour is governed by static acceleration coefficients and predefined inertia scheduling. In contrast, VL-APSO-LS introduces adaptive inertia weight and adaptive acceleration coefficients that respond to fitness progression during the optimisation process. This adaptive learning strategy enables the swarm to dynamically regulate exploration and exploitation, thereby mitigating premature convergence and enhancing convergence stability.

The velocity update mechanism is reformulated to integrate adaptive diversification control and dynamic representation learning, allowing particles to simultaneously adjust their positional search trajectory and subset dimensionality. By coupling adaptive parameter control with variable-length encoding, the proposed method aims to identify compact yet discriminative feature subsets in high-dimensional microarray data. The configuration settings and evaluation parameters used in this study are summarised in Table 2.

3.5. Classification and validation strategy

To evaluate the discriminative quality of the selected feature subsets, four classifiers were employed: KNN, DT, NB, and SVM. These classifiers represent diverse learning paradigms, including distance-based, rule-based, probabilistic, and margin-based approaches, and are also the most widely used in machine learning algorithms for classification (Bokhare & Jha, 2023; Ozcan et al., 2022).

Performance evaluation was conducted using k-fold cross-validation to ensure robust estimation and maximise data utilisation. This approach allows each sample to be used once for validation, thereby reducing

the risk of overfitting and improving the reliability of the reported classification accuracy (Mahesh et al., 2023). It ensures that each sample is used for validation exactly once, helping mitigate overfitting and underfitting.

Beyond empirical comparison, statistical validation was performed using the Wilcoxon signed-rank test and a non-inferiority framework. The Wilcoxon test was employed to assess paired performance differences across folds without assuming normality. The non-inferiority analysis evaluated whether the proposed VL-APSO-LS method performs no worse than the baseline VLPSO-LS beyond a predefined margin ($\delta = 1$ percentage point) at a one-sided significance level of $\alpha = 0.05$. Unlike conventional null-hypothesis significance testing, the non-inferiority framework explicitly evaluates practical equivalence, thereby preventing misleading interpretations of non-significant results. This dual-validation strategy ensures that observed performance improvements are statistically robust and practically meaningful, rather than attributable to sampling variability. The process summary is shown in Table 2.

Tab. 2. Summary of datasets, techniques, and evaluation measures

Component	Description
Datasets	Leukaemia, SRBCT, Colon, Lymphoma, Lung Cancer
Feature selection	VLPSO-LS (baseline), VL-APSO-LS (proposed)
Classifiers	KNN, DT, NB, SVM
Validation	k-fold cross-validation
Statistical Tests	Wilcoxon signed-rank test; Non-inferiority test ($\delta = 1$ pp, $\alpha = 0.05$)
Runs of each experiment	30 times

The evaluation was conducted on five benchmark microarray datasets to assess the robustness and generalisability of the proposed VL-APSO-LS framework across diverse problem characteristics. These datasets differ in terms of dimensionality, sample size, class distribution, and cancer type, thereby providing a comprehensive test environment for feature selection algorithms. Evaluating multiple datasets allows investigation into whether the proposed adaptive optimisation strategy consistently improves performance across different biological domains and data structures, rather than producing results specific to a single dataset.

A stratified 10-fold cross-validation procedure was employed to evaluate the proposed method. For each fold, the dataset was partitioned into training and testing subsets. All preprocessing operations, including normalisation, IG ranking, Symmetric Uncertainty (SU) filtering, and feature selection using VL-APSO-LS, were conducted exclusively on the training subset.

The test subset was not involved in any stage of feature ranking, feature selection, or parameter estimation. The selected feature subset and normalisation parameters obtained from the training data were then applied to the corresponding test subset to evaluate the classifier. This procedure, as shown in Figure 3, prevents information leakage and ensures an unbiased estimation of classification performance. This protocol strictly follows best practices for feature selection evaluation and eliminates the possibility of information leakage between the training and testing partitions.

Due to the stochastic nature of PSO-based optimisation, each experiment was independently repeated 30 times using different random initialisations of particle positions and velocities. The reported results correspond to the average performance obtained across all runs. This repeated-run protocol was adopted to minimise the influence of random variation and to provide a more reliable assessment of algorithm performance.

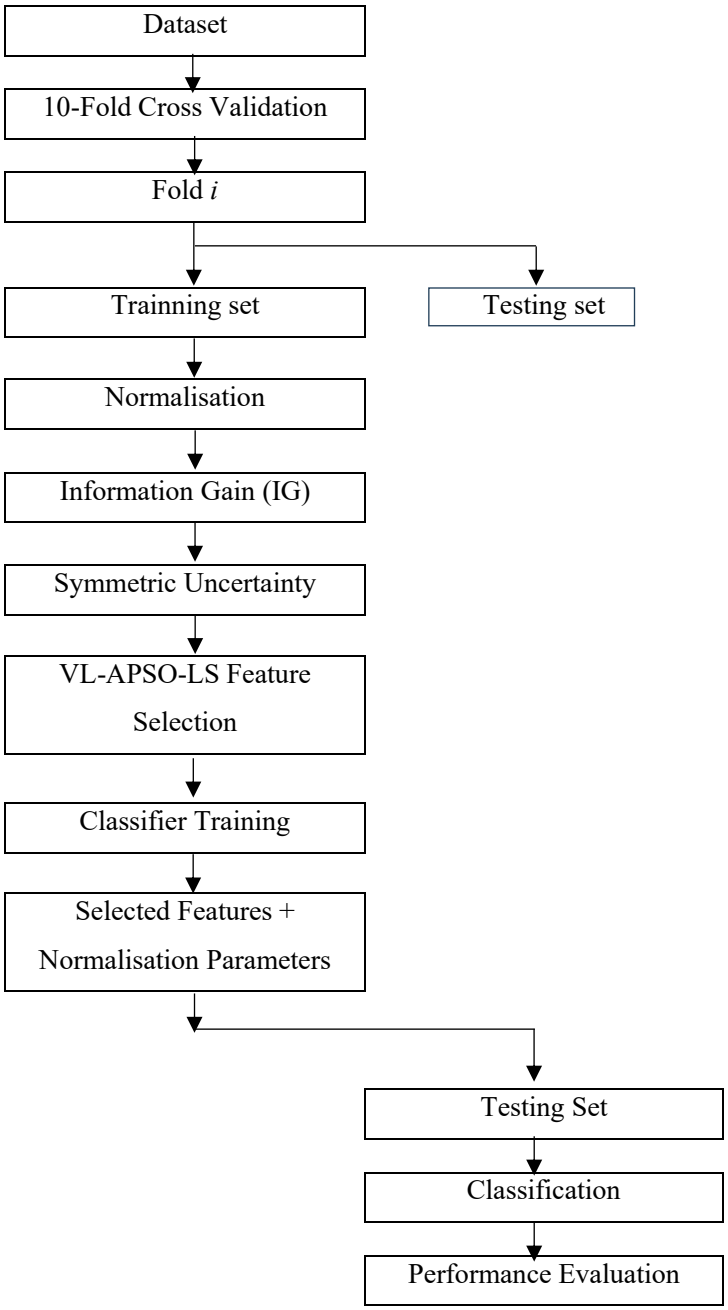


Fig. 3. Validation procedure used in each cross-validation iteration

3.6. Algorithm procedure

Based on the variable-length representation, VLPSO-LS and the proposed VL-APSO-LS allow particles within the population to assume arbitrary lengths smaller than the original problem dimensionality. In this framework, the exemplar serves as a dimension-wise learning reference that guides each particle's velocity update. This mechanism extends the learning process beyond the conventional reliance on personal best (pbest) and global best (gbest) positions. As illustrated in Figure 4, for each particle i and each dimension d, an exemplar index $e_{i,d}$ is assigned to identify the particle whose historical best position serves as the learning source for that specific dimension. This mechanism allows different dimensions of the same particle to learn from different members of the swarm. Such a distributed learning strategy increases population diversity and reduces the risk of premature convergence. Rather than being guided by a single global attractor, the search process is influenced by multiple informative sources throughout the swarm.

Tab. 3. Data structure of particle *i* in the VLPSO algorithm (Tran et al., 2019)

Dimension (*d*):	*1*	*2*	*3*	*4*	*5*	*1*	*2*	*3*	...	*L*
Position (*x*):	0.8	0.3	0.9	0.4	0.1	0.6	0.2	0.7	…	0.2
Velocity (*v*):	0.1	0.2	0.5	0.4	0.1	0.2	0.4	0.3	…	0.2
Exemplar (*e*):	8	7	5	6	2	3	7	8	…	1
Learning Probability (*Pc*) = Eq. 6						**Renew Exemplar Count = 3**				

The exemplar is established during the population initialisation phase, after all particles have determined their respective pbest positions as illustrated in Table 3. Typically, this selection is performed using a fitness-based mechanism such as tournament selection. Subsequently, exemplars are updated adaptively rather than at every iteration. The update is triggered when a particle stagnates for a predefined number of iterations, controlled by the renew exemplar count parameter, or when the learning probability Pci is met. This adaptive update strategy maintains a balance between exploration and exploitation, enhancing the global search capability of the VLPSO algorithm. The overall process of the proposed framework is illustrated in Figure 4, which presents the complete workflow of the variable-length adaptive PSO mechanism.

The learning probability Pc_i determines the likelihood that particle i selects exemplars from other particles rather than learning exclusively from its own experience. Following the comprehensive learning strategy, particles with better rankings are assigned lower learning probabilities, whereas particles with poorer rankings are assigned higher learning probabilities to encourage exploration. The learning probability is computed using:

$$Pc_i = 0.05 + 0.45 \times \frac{\exp\left(\frac{10(rank(i)-1)}{S-1}\right)-1}{\exp(10)-1} \tag{6}$$

Where Pc_i denotes the learning probability of the particle i, $rank(i)$ represents the fitness ranking of the particle i within the swarm, and S denotes the swarm size. The exponential mapping generates a non-linear distribution of learning probabilities within the range [0.05,0.50], allowing highly ranked particles to preserve exploitation behaviour while encouraging lower-ranked particles to increase exploration through exemplar learning. This mechanism helps maintain population diversity and reduces the risk of premature convergence during the optimisation process.

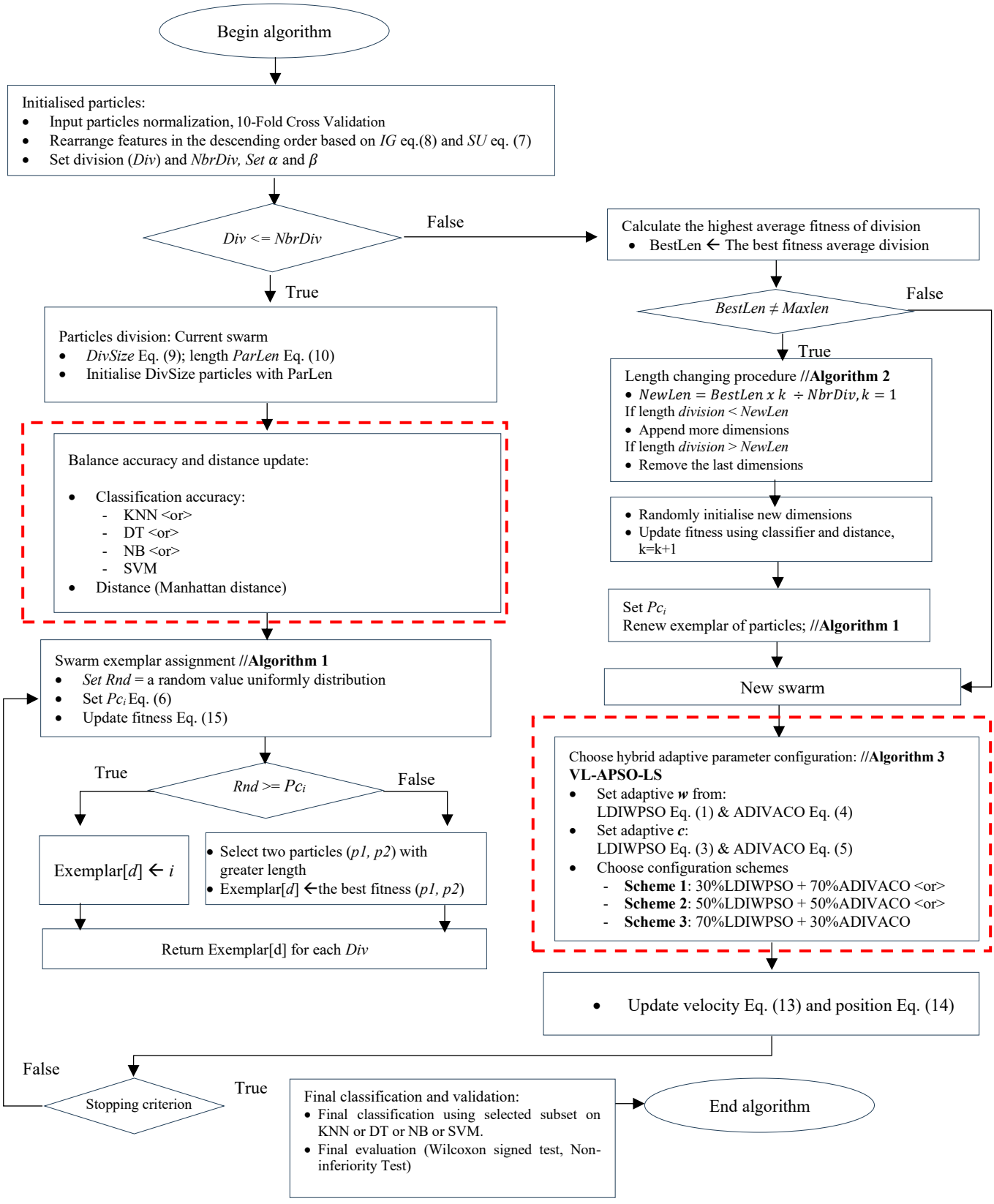


Fig. 4. Overall variable-length adaptive PSO algorithm

Based on Figure 4, the proposed optimisation process begins with the initialisation and swarm division stages. During the preprocessing phase, the input particles are normalised, and the feature set is ranked by relevance using symmetric uncertainty and information gain. The symmetric uncertainty between two variables is defined as:

$$SU(F,C) = \left[\frac{IG(F|C)}{H(F)+H(C)}\right] \tag{7}$$

Where $SU(F,C)$ represents the symmetric uncertainty between features *F* and *C*, *IG* denotes the information gain and H(.) is the entropy function. The information gain used to quantify feature relevance is computed as:

$$IG(F|C) = H(F) - H(F|C) \tag{8}$$

Where $H(F)$ represents the entropy of feature *F* and $H(F,C)$ denotes the conditional entropy of *H* given *C.* These measures are used to rearrange the features in descending order of importance prior to the swarm division process. The swarm is then partitioned into several divisions according to the predefined number of divisions, which determines the division size.

$$DivSize = \frac{PopSize}{NbrDiv} \tag{9}$$

Where *PopSize* denotes the total size of particle in population and NbrDiv represents the number of divisions. For each division, the particle length is determined using the length formulation.

$$ParLen_v = MaxLen * \frac{V}{NbrDiv} \tag{10}$$

Where $ParLen_v$ denotes the updated particle length, $MaxLen$ corresponds to the particle length associated with the maximum length of the division, and *v* denotes the division index.

After the swarm division stage, each subgroup undergoes fitness evaluation based on a combination of classification accuracy and a distance-based criterion. Classification accuracy is obtained from several classifiers, including KNN, DT, NB, and SVM, while feature diversity is measured using the Manhattan distance. These two criteria are integrated through the composite fitness function.

$$fitness = (\gamma.accuracy + (1-\gamma).distance \tag{11}$$

Where fitness denotes the evaluation value of the particle, accuracy represents the classification performance, distance corresponds to the Manhattan distance between feature subsets, and γ controls the balance between the two criteria.

The exemplar selection strategy is then performed as described in Algorithm 1. For each dimension, a particle either retains itself as the learning reference or selects another particle with better fitness performance. The computed fitness values are used for exemplar assignment, division comparison, and learning probability updates, thereby ensuring consistent adaptive behaviour across the swarm.

Based on the average fitness obtained from each division, particle lengths are dynamically adjusted using the structural adaptation mechanism described in Algorithm 2. The length-changing procedure regulates the dimensional expansion or reduction of particles through

$$NewLen = \frac{BestLen\ x\ k}{NbrDiv} \tag{12}$$

Where $NewLen$ denote the updated and previous particle lengths, respectively, and k represents the order length adjustment. During this step, dimensions may be appended or removed to maintain balanced performance across divisions.

Within each iteration, the hybrid adaptive parameter configuration described in Algorithm 3 is applied. The time-varying w is computed using the linear decreasing w formulation of LDIW-PSO using Eq. (1) and c of LDIW-PSO is expressed as Eq. (3). In addition, the adaptive inertia weight mechanism adopted from ADIVACO is expressed as Eq. (4) and the c for ADIVACO is adaptively adjusted using Eq. (5).

Using these adaptive parameters, particle velocities and positions are updated according to the standard PSO learning mechanism. The velocity update rule is defined as

$$v_{id}^{t+1} = \boldsymbol{w_i} \cdot v_{id}^{t} + \boldsymbol{c_i} \cdot r_{id} \cdot pbest_{f_{i(d)}}^{t} - x_{id}^{t} \tag{13}$$

Where v_{id}^{t+1} represents the current velocity of particle *i* at iteration *t*, w_i denotes the inertia weight of particle *i*, v_{id}^{t} are the velocity of particle *i* at iteration *t*, c_i is the acceleration coefficient of particle *i*, r_{id} are random numbers in the interval [0,1], $pbest_{f_{i(d)}}^{t}$ denotes the personal best position, and x_{id}^{t} denotes the position of particle *i* at iteration *t*. The particle position is then updated according to

$$x_{id}^{t+1} = x_{id}^{t} + v_{id}^{t+1} \tag{14}$$

Where x_{id}^{t+1} represents the current position of particle *i*.

To simultaneously optimise classification performance and feature diversity, a composite fitness function is employed. The fitness value is defined as:

$$fitness = (\gamma \times accuracy) + ((1-\gamma) \times distance) \tag{15}$$

Where *fitness* is the overall quality measure of a particle, *accuracy* denotes the classification accuracy achieved by the selected feature subset, *distance* represents the Manhattan distance used to evaluate feature diversity, and $\gamma \in [0,1]$ is a weighting parameter that determines the relative importance of the two objectives. The resulting fitness values are subsequently used to rank particles within the swarm. Based on these rankings, the Pc_i of each particle is computed to regulate the exemplar selection mechanism. Particles with superior fitness rankings are assigned lower learning probabilities to preserve exploitation behaviour, whereas particles with poorer fitness rankings receive higher learning probabilities to encourage exploration.

The iterative process continues until the stopping criterion is satisfied. Once convergence is achieved, the best-performing particle is selected as the final feature subset. The selected features are subsequently evaluated using multiple classifiers, including KNN, DT, NB, and SVM. Complementing the conceptual workflow, Table 4. presents the complete algorithmic realisation of the proposed framework.

Tab. 4. Pseudocode for VLPSO and VL-APSO-LS

Algorithm 1: Exemplar Assignment
Input: Particle i
Output: Exemplar for each dimension of Particle *i*

```
1    begin
2    L ← the length of particle i;
3    for d = 1 to L do
4    Rnd ← a random value drawn from a uniform distribution;
5    PCi ← Pc of particle i;
6     if (Rnd >= PCi) then
7          exemplar[d] ← i;
8       else
9          p1 ← randomly pick a particle that is
                   different from i and has a length
                   longer than d;
10         p2 ← randomly pick a particle that is
                   different from i and p1 and has a
                   length longer than d;
11          **// Calculate fitness for p1 and p2 using classifier**
12          if (Model == 'KNN') then
13             fitness_p1 ← CrossValidation(CalculateKNNAccuracy(p1), k=10);
14             fitness_p2 ← CrossValidation(CalculateKNNAccuracy(p2) k=10);
15          else if (Model == 'DT') then
16             fitness_p1 ← CrossValidation(CalculateDTAccuracy(p1),k=10);
17             fitness_p2 ← CrossValidation(CalculateDTAccuracy(p2), k=10);
18          else if (Model == 'NB') then
19             fitness_p1 ← CrossValidation(CalculateNBAccuracy(p1),k=10);
20             fitness_p2 ← CrossValidation(CalculateNBAccuracy(p2), k=10);
21          else if (Model == 'SVM') then
22             fitness_p1 ← CrossValidation(CalculateSVMAccuracy(p1),k=10);
23             fitness_p2 ← CrossValidation(CalculateSVMAccuracy(p2), k=10);
```

Tab. 4. Pseudocode for VLPSO and VL-APSO-LS, continued

Algorithm 1: Exemplar Assignment, continued

```
24          end
25          **// Compare fitness and assign exemplar**
26          if (fitness_p1 > fitness_p2) then
27              exemplar[d] ← p1;
28          else
29              exemplar[d] ← p2;
30          end
31        end
32    end
33    Return exemplar;
34  end
```

Algorithm 2: Length Changing Procedure

Input: Current swarm
Output: New swarm

```
1 begin
2 NbrDiv ← Number of divisions of the current swarm;
3 MaxLen ← Max length of particles in the current swarm;
4 Calculate the average fitness of each division;
5 BestLen ← Particles' length of the best division;
6     if (BestLen ≠ MaxLen) then
7         k ← 1;
8         for each division v (different from the best division) do
9             NewLen ← BestLen × k ÷ NbrDiv;
10            if (Length of particles in v < NewLen) then
11                Append more dimensions to particles in v to have NewLen dimensions;
12                Randomly initialise the new dimensions;
13                // Calculate fitness using classification models
14                if (Model == 'KNN') then
15                    fitness ← CalculateKNNAccuracy(particle);
16                else if (Model == 'DT') then
17                    fitness ← CalculateDTAccuracy(particle);
18                else if (Model == 'NB') then
19                    fitness ← CalculateNBAccuracy(particle);
20                else if (Model == 'SVM') then
21                    fitness ← CalculateSVMAccuracy(particle);
22                end
23                // Calculate distance (e.g., Manhattan Distance)
24                distance ← CalculateDistance(particle);
25                // Combine accuracy and distance for final fitness
26                finalFitness ← (γ * accuracy) + ((1 - γ) * distance);
27                // Update particle fitness
28                UpdateFitness(particle, finalFitness);
29                k = k + 1;
30            else
31                if (Length of particles in v > NewLen) then
32                    Remove the last dimensions of particles in v to have NewLen dimensions;
33                    // Recalculate fitness after dimension removal
34                    fitness ← RecalculateFitness(particle);
35                    k = k + 1;
36                end
37            end
38        end
39    end
40    Calculate Pci for all particles using Eq. (6);
41    Renew exemplar of particles; // Algorithm 1
42    Return swarm;
43 end
```

Tab. 4. Pseudocode for VLPSO and VL-APSO-LS, continued

```
Algorithm 3: Hybrid Adaptive Parameter Configuration (VL-APSO-LS)
Input : swarm (positions x, velocities v, exemplars), iteration t, maxIter, Scheme ∈ {1,2,3}
Output: swarm (updated velocities and positions)

begin
    // Step 1: compute adaptive candidates from two strategies
    w_L ← Compute_w_LDIWPSO(t)                    // Eq. (1)
    c_L ← Compute_c_LDIWPSO(t)                    // Eq. (3)
    w_A ← Compute_w_ADIVACO(t)                    // Eq. (4)
    c_A ← Compute_c_ADIVACO(t)                    // Eq. (5)

    // Step 2: choose ONE configuration scheme (OR)
    if (Scheme == 1) then
        a ← 0.30                                  // weight for LDIWPSO
        b ← 0.70                                  // weight for ADIVACO
    else if (Scheme == 2) then
        a ← 0.50
        b ← 0.50
    else if (Scheme == 3) then
        a ← 0.70
        b ← 0.30
    end if

    // Step 3: hybrid adaptive parameters (single c, assume c1 = c2 = c)
    w ← a * w_L + b * w_A
    c ← a * c_L + b * c_A

    // Step 4: update velocity & position (exemplar-based / comprehensive learning)
    for each particle i in swarm do
        L_i ← length(particle i)
        for d = 1 to L_i do
            r ← rand(0,1)
            p ← exemplar_i[d]                     // exemplar index for dim d
            v_i[d] ← w * v_i[d] + c * r * ( x_p[d] − x_i[d] )   // Eq. (13)
            x_i[d] ← x_i[d] + v_i[d]              // Eq. (14)
        end for
        ApplyBoundsOrBinarization(x_i)
    end for
    Return swarm
end
```

Based on Table 4, Algorithm 1 formalises the exemplar assignment mechanism at the dimension level. Algorithm 2 implements the variable-length adaptation mechanism. Algorithm 3 governs the hybrid adaptive parameter configuration. At each iteration, candidate inertia weights and acceleration coefficients are computed separately using the LDIW-PSO and ADIVACO parameter strategies. One of three predefined configuration schemes is then selected (Scheme 1, Scheme 2, or Scheme 3), assigning different contribution weights to each strategy. The final adaptive parameters are obtained by combining these weights and are subsequently used in the exemplar-based velocity and position update equations. Through this hybrid parameter control mechanism, the algorithm dynamically balances exploration and exploitation while preserving structural adaptability.

3.7. Experimental design and method configuration

This section describes the experimental configuration used to evaluate the proposed hybrid adaptive strategy under controlled and reproducible conditions. The proposed VL-APSO-LS method integrates adaptive parameter control with dynamic particle-length adjustment to improve feature selection in high-dimensional microarray gene-expression datasets. The framework combines mechanisms inspired by LDIW-PSO, which

employs time-varying inertia weight and acceleration coefficients, and ADIVACO, which introduces adaptive diversification control. Table 5. summarises the parameter-control components used in both the baseline and comparative methods.

Tab. 5. Summary of control components adopted in the development of VL-APSO-LS

Method	Particle Representation	Inertia Weight	Acceleration Factor	Velocity Update
LDIW-PSO	Fixed	Time-varying	Time-varying	Conventional
ADIVACO	Fixed	Adaptive	Adaptive	Conventional
VLPSO-LS	Dynamic	Time-varying	Static	Comprehensive
VL-APSO-LS	Dynamic	Adaptive	Adaptive	Comprehensive

Unlike VLPSO-LS, which employs partially adaptive mechanisms, VL-APSO-LS incorporates a dynamic particle representation and adaptive inertia weights and acceleration coefficients that respond to particle performance across swarm divisions. The relative contributions of the LDIW-PSO and ADIVACO components are implemented through weighted integration within the velocity update formulation. This hybridisation strategy aims to regulate the exploration-exploitation balance more flexibly in high-dimensional search spaces, resulting in three exploration-exploitation configurations:

- Scheme 1 (30% LDIWPSO + 70% ADIVACO): This scheme emphasises adaptive diversification control of ADIVACO by prioritising exploitation and convergence stability, while mitigating oscillatory search behaviour.
- Scheme 2 (50% LDIWPSO + 50% ADIVACO): This configuration balances global exploration and local exploitation to achieve stable convergence and consistent feature subset quality.
- Scheme 3 (70% LDIWPSO + 30% ADIVACO): This configuration increases the influence of linearly decreasing inertia weight, encouraging broader search diversification during early iterations at the potential expense of late-stage fine-tuning.

The three schemes were predefined before experimentation and were evaluated independently without selecting a scheme based on test performance. Similarly, classifier parameters followed standard settings commonly adopted in previous studies. The proportional configurations (30-50-70%) were selected to represent low, balanced, and high dominance scenarios of each strategy, enabling controlled analysis of exploration-exploitation dynamics while maintaining manageable hyperparameter dimensionality. This design allows attribution of performance differences specifically to the exploration-exploitation balance rather than to unrelated parameter variations.

A sensitivity analysis was conducted by comparing Schemes 1, 2, and 3 across all benchmark datasets. The results indicate that increasing the contribution of ADIVACO generally improves exploration capability and classification performance, whereas higher LDIWPSO dominance tends to promote convergence stability. The balanced configuration (Scheme 2) provides a favourable trade-off between classification accuracy, feature subset compactness, and optimisation stability as shown in Table **6**.

3.7.1. Wilcoxon signed-rank trend analysis

In this study, the Wilcoxon signed-rank test was employed to assess the performance differences between VL-APSO-LS and the baseline VLPSO-LS. This test evaluated the median differences in fitness and classification accuracy across paired results from each dataset and cross-validation fold. The procedure was carried out as follows: First, the differences $d_i = X_i - Y_i$, for $i = 1,2,\dots,k$, were computed, where d_i represents the difference in either fitness or accuracy. Zero differences ($d_i = 0$) were excluded from the analysis. The absolute differences $|d_i|$were then ranked, with average ranks assigned in the case of ties. The differences were noted, and the rank sums were calculated. Specifically, W^+denotes the sum of ranks with positive d_i, and W^- represents the sum of ranks with negative d_i. The test statistic W is determined as the minimum of W^+ and W^-. The decision rule is as follows: if $p \leq 0.05$, a significant difference is found between VL-APSO-LS and VLPSO-LS; if $p > 0.05$, no significant difference is detected.

The primary focus was on capturing the trend in performance change, as reflected in the Wilcoxon statistics. Specifically, a trend of increasing values W^+indicates an improvement, while a trend of decreasing W^-sign indicates consistent degradation. The trend indicators (↑, ↓, ≈, Mixed) provide a clear representation of

directional shifts in performance across the datasets, indicating whether the proposed method generally improves, degrades, or maintains performance comparable to the baseline.

3.7.2. Non-inferiority evaluation procedure

Non-inferiority testing inverts the typical null hypothesis logic. Rather than asking whether two methods differ, it asks whether the new method is no worse than the baseline, particularly when the new method offers additional advantages such as lower cost or reduced complexity within a pre-specified margin (δ). This margin represents the maximum tolerable loss in performance that would still render the new algorithm acceptable. For instance, if δ = 2% accuracy, then demonstrating that VL-APSO-LS is within 2% of VLPSO establishes non-inferiority. If the confidence interval around the performance difference lies entirely above $-\delta$, non-inferiority is confirmed (Gibbons & Chakraborti, 2003). Superiority analysis assesses whether a new method achieves statistically significant improvement over an existing process (Stefanos et al., 2020; Ravenzwaaij et al., 2019).

This evaluation was conducted using a predefined non-inferiority margin (δ), which served as a practical threshold to ensure that the proposed method achieved results at least comparable to the baseline. The hypotheses tested were: H_0: $\mu_0 \leq -\delta$ (indicating that VL-APSO-LS is inferior) and H_1: $\mu_0 > -\delta$ (indicating that VL-APSO-LS is non-inferior). The sample statistics used in this analysis were the mean difference $\bar{d}$, calculated as $\frac{1}{n}\sum_i d_i$, and the standard deviation S_d, which was derived from the formula $S_d = \sqrt{\frac{1}{n-1}\sum_i (d_i - \bar{d})^2}$. The standard error (*SE*) was then calculated as $SE = \frac{S_d}{\sqrt{n}}$. The test statistic, t_{NI}, was computed using the formula $t_{NI} = \frac{\bar{d}+\delta}{SE}$.

Where n = 3, for the three schemes (Scheme 1, Scheme 2, and Scheme 3), which the decision rule was based on the calculated t_{NI}: if $t_{NI} > t_{(1-\alpha,n-1)}$, non-inferiority was concluded. The test statistic followed a *t*-distribution with $n-1$ degrees of freedom of the three schemes (Scheme 1, Scheme 2, and Scheme 3) were calculated as *df* = 3 - 1 = 2. If the 95% confidence interval lower bound was greater than zero $\left(LB_{95\%} = \bar{d} - t_{1-\alpha,n-1} \times SE\right) > 0$, superiority was concluded. This approach enables a robust evaluation of whether the proposed method is statistically non-inferior to the baseline and, if applicable, superior.

4. RESULTS AND DISCUSSION

4.1. Classification performance on test data

To further examine the impact of different hybrid configurations in the proposed VL-APSO-LS method, a comprehensive fitness comparison was conducted. The experiments were performed on five widely used gene-expression microarray datasets: Colon, SRBCT, Lymphoma, Leukaemia, and Lung cancer. Performance was evaluated using four classifiers: KNN, DT, NB, and SVM. The analysis focuses on fitness values, statistical validation, convergence behaviour, classification accuracy, and feature-selection effectiveness. Table 5. summarises the classification accuracy obtained on unseen test data across the five benchmark datasets using the four classifiers.

A comprehensive comparison between the baseline VLPSO-LS and the proposed VL-APSO-LS, summarised in Table 5, highlights their performance across five benchmark gene-expression datasets. The comparison includes feature subset size, mean fitness, classification accuracy, and the best-performing classifier. Overall, VL-APSO-LS consistently demonstrates superior or competitive classification accuracy while effectively controlling feature dimensionality. The Wilcoxon trend test, derived from the Wilcoxon signed-rank test, indicates statistically significant improvements across several configurations.

Tab. 6. Classification results that focus on test accuracy

Dataset	Method	Size	Mean		Best Classifier	Wilcoxon Trend
			Fitness	Accuracy		
Colon	VLPSO-LS	491	77.74	83.48	SVM	
	Scheme 1	86	79.74	85.85	SVM	↑
	Scheme 2	87	80.40	85.35	SVM	↑
	Scheme 3	83	80.72	86.07	SVM	↑
SRBCT	VLPSO-LS	74	89.59	100	NB	
	Scheme 1	70	89.75	100	KNN	≈
	Scheme 2	71	89.80	100	KNN	≈
	Scheme 3	72	89.80	100	KNN	≈
Lymphoma	VLPSO-LS	486	87.65	91.9	SVM	
	Scheme 1	303	99.38	97.67	SVM	↑
	Scheme 2	299	99.44	97.69	SVM	↑
	Scheme 3	300	99.45	97.4	SVM	↑
Leukaemia	VLPSO-LS	119	87.64	96.75	SVM	
	Scheme 1	850	91.56	95.88	SVM	↑
	Scheme 2	840	88.48	95.25	NB	↑
	Scheme 3	854	91.64	96.77	SVM	↑
Lung	VLPSO-LS	2136	84.01	93.97	SVM	
	Scheme 1	2202	82.94	94.14	SVM	↑
	Scheme 2	2112	82.98	95.62	SVM	↑
	Scheme 3	2114	83.00	93.89	SVM	↓

1. In the Colon dataset, all VL-APSO-LS schemes significantly reduce the number of selected features from 491 to fewer than 90, while improving classification accuracy from 83.48% to a maximum of 86.07%. This result indicates that the adaptive optimisation mechanism successfully removes redundant features and enhances the discriminative capability of the selected subset.
2. In the Lymphoma dataset, A similar pattern is observed where VL-APSO-LS reduces the number of selected features by approximately 38% compared with the baseline while achieving classification accuracies exceeding 97%. Notably, Scheme 2 achieves the highest accuracy (97.69%**)** with only 299 selected features, demonstrating an effective balance between dimensionality reduction and predictive performance.
3. In the Leukaemia dataset, the number of selected features increases under VL-APSO-LS, although the resulting classification accuracy remains comparable to or slightly higher than that of the baseline method. This observation suggests that, for datasets with complex class boundaries, retaining additional informative features may improve classification reliability. Importantly, the improvement in accuracy indicates that the additional features provide useful information rather than introducing redundancy.
4. In the SRBCT**,** all methods achieve perfect classification accuracy (100%), indicating that the dataset is inherently well-separated. Consequently, VL-APSO-LS primarily yields modest feature reduction without degrading predictive performance, demonstrating robustness and stability.
5. In the lung cancer dataset, Schemes 1 and 2 achieve modest improvements in classification accuracy (up to 95.62%), whereas Scheme 3 exhibits a slight performance decline despite maintaining a similar feature subset size. This behaviour suggests that excessively aggressive or imbalanced update proportions may negatively affect generalisation performance, particularly for heterogeneous datasets.

Across all datasets, SVM emerges as the most effective classifier, frequently achieving the best classification performance, especially when combined with VL-APSO-LS. This finding highlights the strong compatibility between margin-based classifiers and adaptive feature-selection strategies in high-dimensional genomic data with limited samples.

Figure 5. presents a comparative analysis of classification accuracy across four optimisation schemes (VLPSO-LS, Scheme 1, Scheme 2, and Scheme 3). Overall, Scheme 2 consistently achieves the highest classification accuracy across classifiers, followed by Scheme 1 and Scheme 3, whereas the baseline VLPSO-LS generally performs the worst.

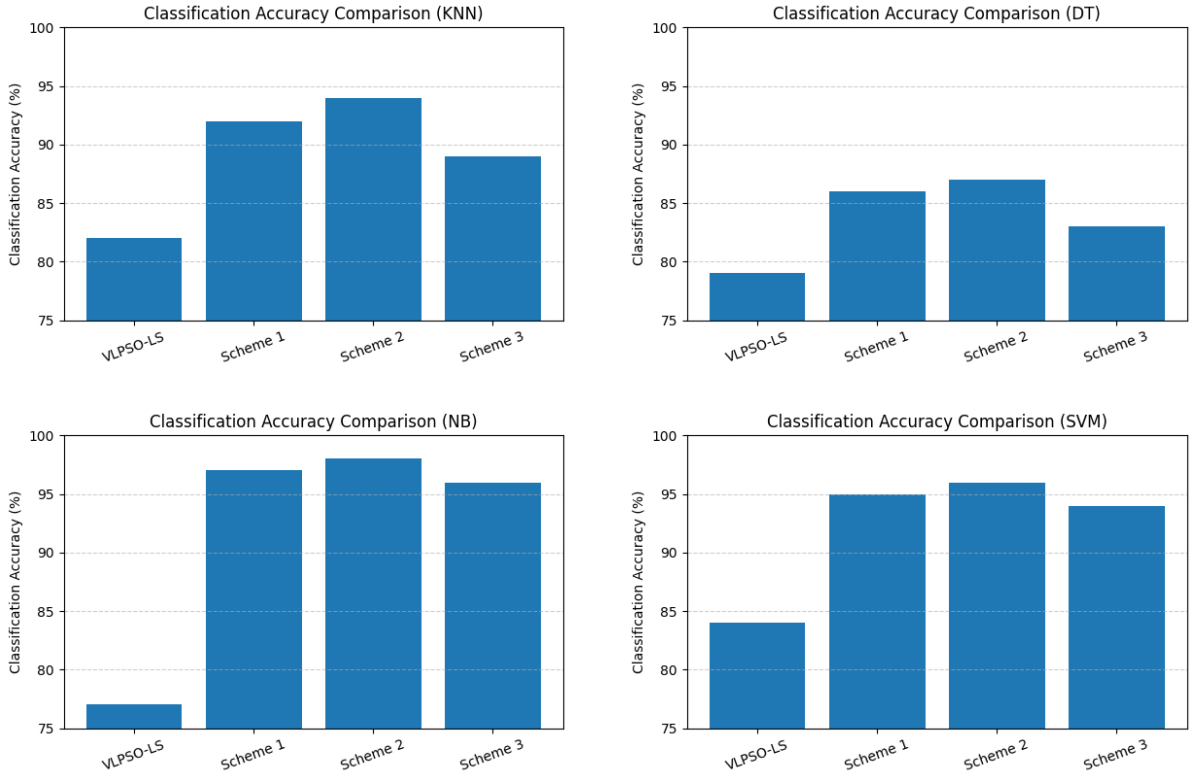


Fig. 5 The classification result comparison

As illustrated in Figure 5, the performance improvement is particularly evident for the NB and SVM classifiers, where Scheme 2 demonstrates clear and stable accuracy gains. Although all classifiers benefit from the enhanced optimisation schemes, NB achieves the highest overall accuracy, followed by SVM, indicating that probabilistic and margin-based classifiers respond particularly well to the improved feature selection strategy. These findings demonstrate the robustness and effectiveness of the proposed optimisation variants in improving classification performance across different learning models. In addition, the convergence behaviour illustrated in Figure 5 provides evidence of the algorithm's stability across different configuration schemes, highlighting the exploration-exploitation characteristics introduced by varying the relative contributions of LDIWPSO and ADIVACO.

To jointly evaluate classification performance and feature compactness, the Accuracy-to-Feature Ratio (AFR) was employed as a composite efficiency indicator for each method-classifier combination (J. Li et al., 2018; Xue et al., 2013):

$$AFR = \frac{Accuracy(\%)}{Feature\ size} \tag{15}$$

Tab. 7**. Performance comparison of VLPSO-LS and VL-APSO-LS schemes in terms of accuracy and feature reduction**

Scheme	Avg. accuracy	Avg. Feature size	AFR	Analysis
VLPSO-LS	92.64	275	0.3369	High accuracy, but the highest feature count
Scheme 1	94.50	248	0.3811	The most efficient in balancing accuracy and feature size
Scheme 2	94.39	250	0.3775	Strong balance between accuracy and feature reduction.
Scheme 3	94.65	256	0.3697	While it improves accuracy, it sacrifices efficiency in feature reduction

As shown in Table 7, the baseline VLPSO-LS achieves a competitive average accuracy of 92.64%, but at the cost of selecting the largest average feature subset (275 features), indicating limited efficiency in dimensionality reduction. Among the proposed configurations, Scheme 1 demonstrates the highest efficiency. It achieves the second-highest classification accuracy (94.50%) while maintaining the smallest feature subset,

yielding the highest AFR (0.3811). Scheme 2 provides the most balanced performance, offering a strong compromise between classification accuracy and feature compactness. With a competitive AFR of 0.3775, Scheme 2 is particularly suitable for scenarios where both predictive performance and dimensionality reduction are equally important. As illustrated in Figure 6, Scheme 2 also exhibits the most stable and consistent optimisation behaviour across datasets, suggesting a well-balanced exploration–exploitation mechanism during the optimisation process.

In contrast, Scheme 3 achieves the highest average accuracy (94.65%), but with reduced efficiency. Its larger feature subset results in a lower AFR (0.3697), indicating that the improvement in accuracy comes at the expense of increased dimensionality. Although Scheme 3 achieves superior predictive performance, the additional accuracy gain comes at the cost of selecting more features. Since AFR simultaneously considers classification performance and feature subset compactness, the increase in feature count can outweigh the relatively modest improvement in accuracy. This suggests that Scheme 3 prioritises maximising predictive performance, whereas Schemes 1 and 2 provide a more balanced trade-off between classification accuracy and dimensionality reduction. Consequently, the higher accuracy of Scheme 3 does not necessarily translate into superior feature selection efficiency when evaluated using AFR.

Finally, although VLPSO-LS achieves relatively high classification accuracy, it retains more features than the proposed variants, resulting in a lower AFR. This suggests that the baseline method is less efficient in reducing dimensionality despite maintaining strong predictive performance.

4.2. Statistical validation: Wilcoxon and non-inferiority analysis

The Wilcoxon signed-rank test was employed to examine paired performance differences between VL-APSO-LS and VLPSO-LS across classifiers and datasets. Given the limited number of paired observations (n = 4 classifiers per dataset), the test was primarily used to assess the directional trend of performance changes rather than to establish strict statistical significance. Therefore, the Wilcoxon results were interpreted as directional indicators of comparative performance. Furthermore, the performance differences observed between the methods were generally modest, reducing the likelihood of obtaining statistically significant results under conventional hypothesis testing. Consequently, the Wilcoxon analysis was interpreted as an indicator of performance tendency (improvement, equivalence, or decline) rather than as the sole criterion for method comparison. Accordingly, the resulting Wilcoxon statistics are summarised in Table 8 using trend indicators (↑, ↓, ≈, Mixed), reflecting whether the proposed method generally improves, degrades, or maintains comparable performance relative to the baseline. In this context, a mixed trend indicates that neither positive nor negative performance differences consistently dominate across the evaluated observations, suggesting variability in the comparative behaviour of the two methods. Such results imply that the effectiveness of the proposed feature selection strategy may depend on classifier characteristics and dataset-specific properties.

To provide a more comprehensive assessment, the Wilcoxon trend analysis was complemented by non-inferiority and superiority tests, which are better suited for evaluating practical performance differences when observed improvements are relatively small.

Tab. 8. Result validation on the Wilcoxon test trend and non-inferiority test

Cancer Data	Classifier	Classification Accuracy			Fitness result		
		Wilcoxon Trend	Non-inferiority	Superiority	Wilcoxon Trend	Non-inferiority	Superiority
Colon	KNN	↓	No	No	↑	Yes	Yes
	DT	↑	Yes	No	↑	Yes	Yes
	NB	↑	Yes	Yes	↑	Yes	Yes
	SVM	↑	Yes	Yes	↑	Yes	Yes
SRBCT	KNN	↑	Yes	Yes	↑	Yes	Yes
	DT	↓	Yes	No	↑	Yes	Yes
	NB	↓	No	No	↑	Yes	Yes
	SVM	↑	Yes	Yes	Mixed	Yes	No
Lymphoma	KNN	↑	Yes	Yes	Mixed	Yes	No
	DT	Mixed	No	No	↑	Yes	Yes
	NB	↑	Yes	Yes	↑	Yes	Yes
	SVM	↑	Yes	Yes	↑	Yes	Yes
Leukaemia	KNN	≈	Yes	No	↑	Yes	Yes
	DT	↓	No	No	↑	Yes	Yes
	NB	Mixed	Yes	No	↑	Yes	Yes
	SVM	Mixed	No	No	↑	Yes	Yes
Lung cancer	KNN	↓	No	No	↓	Yes	No
	DT	Mixed	No	No	Mixed	Yes	No
	NB	Mixed	Yes	No	Mixed	Yes	No
	SVM	Mixed	Yes	No	↓	Yes	No

Across all datasets, the proposed VL-APSO-LS method demonstrated strong improvements in accuracy and fitness, particularly with SVM and NB classifiers. While KNN and DT showed mixed or decreasing trends in some datasets, VL-APSO-LS often outperformed the baseline, yielding significant performance improvements.

1. Colon Dataset: The Wilcoxon trend analysis indicates consistent accuracy improvements across all classifiers. NB and SVM achieved both non-inferiority and superiority, demonstrating statistically meaningful improvements over the baseline. DT achieved non-inferiority but not superiority, while KNN failed to meet either criterion, indicating relatively weaker performance. In terms of fitness, all classifiers showed an increasing trend, although KNN again did not reach superiority. These results suggest that VL-APSO-LS provides substantial improvements, particularly when combined with SVM and NB classifiers.
2. SRBCT Dataset: KNN showed consistent improvements in both accuracy and fitness, achieving both non-inferiority and superiority. DT and NB showed declining accuracy, although DT remained non-inferior. SVM displayed a mixed trend, indicating variability across cross-validation folds. For fitness results, most classifiers improved, although SVM showed some instability. Overall, KNN and SVM demonstrated the most reliable performance improvements.
3. Lymphoma Dataset: KNN, NB, and SVM exhibited increasing trends in classification accuracy. NB and SVM achieved both non-inferiority and superiority, confirming the effectiveness of VL-APSO-LS on this dataset. DT displayed a mixed trend with non-inferiority but no superiority. Fitness results similarly showed improvements for NB and SVM, highlighting the consistent effectiveness of the proposed optimisation method.
4. Leukaemia Dataset: KNN exhibited comparable performance (≈) relative to the baseline, achieving non-inferiority but not superiority. NB and SVM showed mixed trends in accuracy, although NB achieved non-inferiority. DT showed a decreasing trend in accuracy and did not satisfy the non-inferiority criterion. For fitness results, both NB and SVM demonstrated non-inferiority and superiority, suggesting that the proposed method remains effective despite the dataset's complex class distribution.
5. Lung Cancer Dataset: The Lung cancer dataset proved to be the most challenging. KNN showed decreasing trends in both accuracy and fitness, without achieving non-inferiority or superiority. DT, NB, and SVM displayed mixed trends, although non-inferiority was still achieved in several cases. These findings indicate that VL-APSO-LS struggles to achieve consistent improvements on this highly heterogeneous dataset, although its performance remains comparable to the baseline.

These findings indicate that VL-APSO-LS struggles to achieve consistent improvements on this highly heterogeneous dataset, although its performance remains comparable to the baseline. The mixed Wilcoxon trends observed primarily for KNN and Decision Tree indicate that performance differences between VL-APSO-LS and VLPSO-LS were not consistently oriented across the evaluated datasets and classifier configurations. In some cases, the proposed method achieved superior classification performance, whereas in others the baseline method remained competitive. This variability may be attributed to the sensitivity of KNN and Decision Tree classifiers to local data distributions, small sample sizes, and variations in the selected feature subsets, which are common characteristics of high-dimensional microarray datasets. Furthermore, KNN relies heavily on distance calculations, while Decision Tree performs hierarchical partitioning of the feature space; consequently, both classifiers are more susceptible to dataset-specific characteristics than SVM and NB, which demonstrated more consistent improvements. Therefore, the mixed Wilcoxon trends should be interpreted as classifier-dependent variability rather than evidence of systematic performance degradation, suggesting that the effectiveness of the proposed optimisation strategy depends, in part, on the interaction between the selected feature subsets and the underlying classification model.

Although the Wilcoxon trend analysis reveals variability across datasets and classifiers, the overall evidence indicates that VL-APSO-LS maintains robust performance relative to the baseline VLPSO-LS. To further strengthen the statistical interpretation, additional non-inferiority and superiority analyses were conducted, as illustrated in Figure 6.

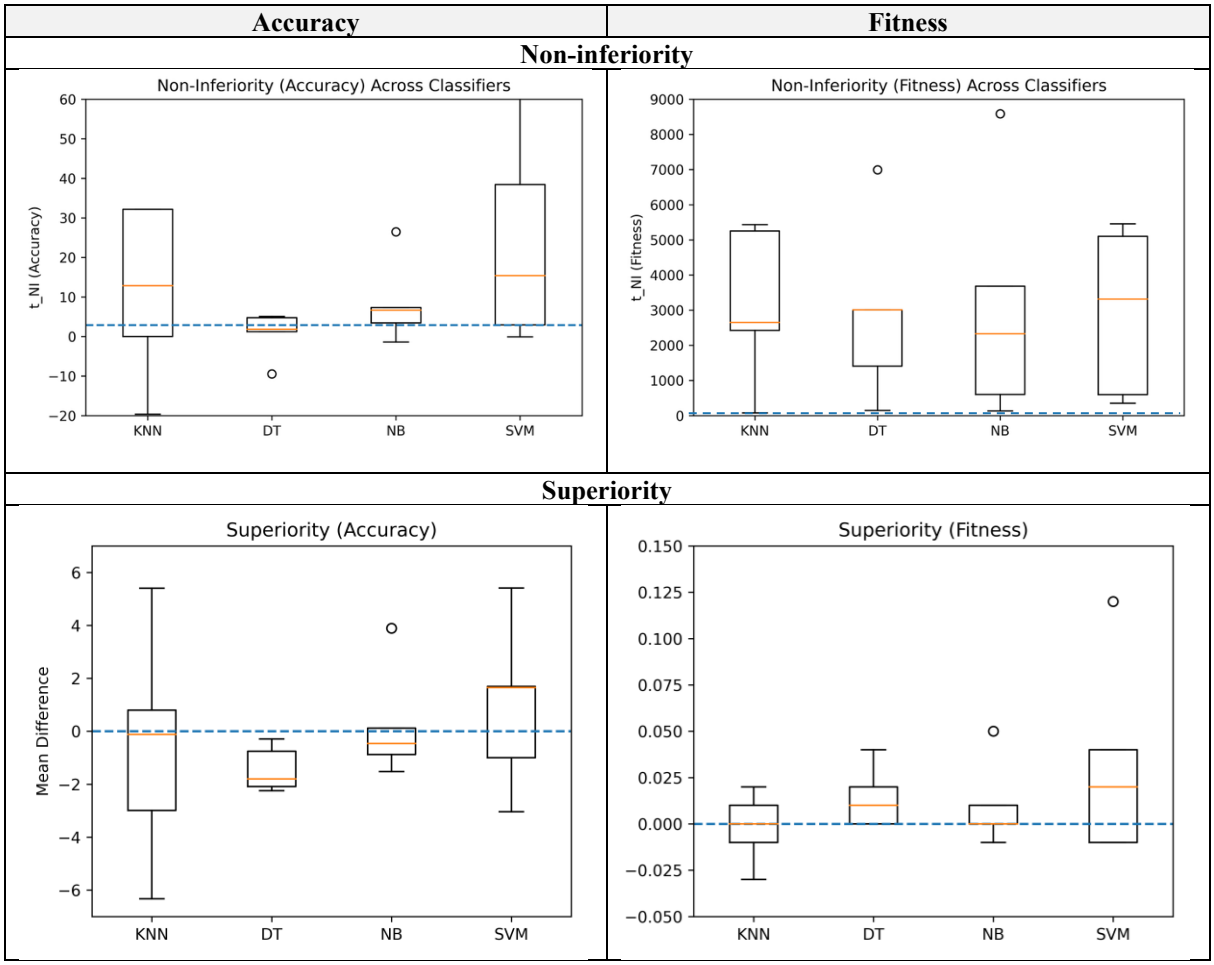


Fig. 6. Non-inferiority and superiority analysis of classification accuracy and fitness across classifiers

The boxplot distributions show limited dispersion around the medians, particularly for SVM and NB, suggesting stable optimisation outcomes with controlled variance. The non-inferiority analysis indicates that VL-APSO-LS consistently satisfies the predefined performance margin across most classifiers for both classification accuracy and fitness, as shown in Figure 6. In particular, SVM demonstrates the most consistent non-inferiority behaviour, followed by NB, suggesting strong generalisation stability under margin-based and

probabilistic learning paradigms. KNN exhibits moderate support for non-inferiority, whereas DT shows comparatively less consistent margins.

The superiority analysis provides additional insight into performance improvements beyond statistical equivalence. Superiority is observed more frequently in fitness values than in classification accuracy, indicating that the proposed optimisation mechanism primarily enhances solution quality and search stability before translating into marginal improvements in predictive performance. Among the classifiers, SVM again exhibits the most consistent superiority patterns in both accuracy and fitness, highlighting the strong synergy between adaptive feature optimisation and margin-based classification. NB also demonstrates favourable superiority trends across several datasets, whereas DT and KNN show more heterogeneous behaviour.

4.3. Performance analysis and practical implications

4.3.1. Convergence behaviour analysis

To further evaluate the optimisation performance of the proposed VL-APSO-LS algorithm, a convergence analysis was conducted on five benchmark microarray datasets: Colon, SRBCT, Lymphoma, Leukaemia, and Lung. The convergence behaviour reflects the algorithm's ability to efficiently explore and exploit the search space while improving fitness values over iterations. Figure 7 illustrates the convergence characteristics of VL-APSO-LS compared to LDIW-PSO, ADIVACO, and VLPSO-LS. The objective of this analysis is to assess not only the final fitness value achieved but also the convergence speed and stability of each method.

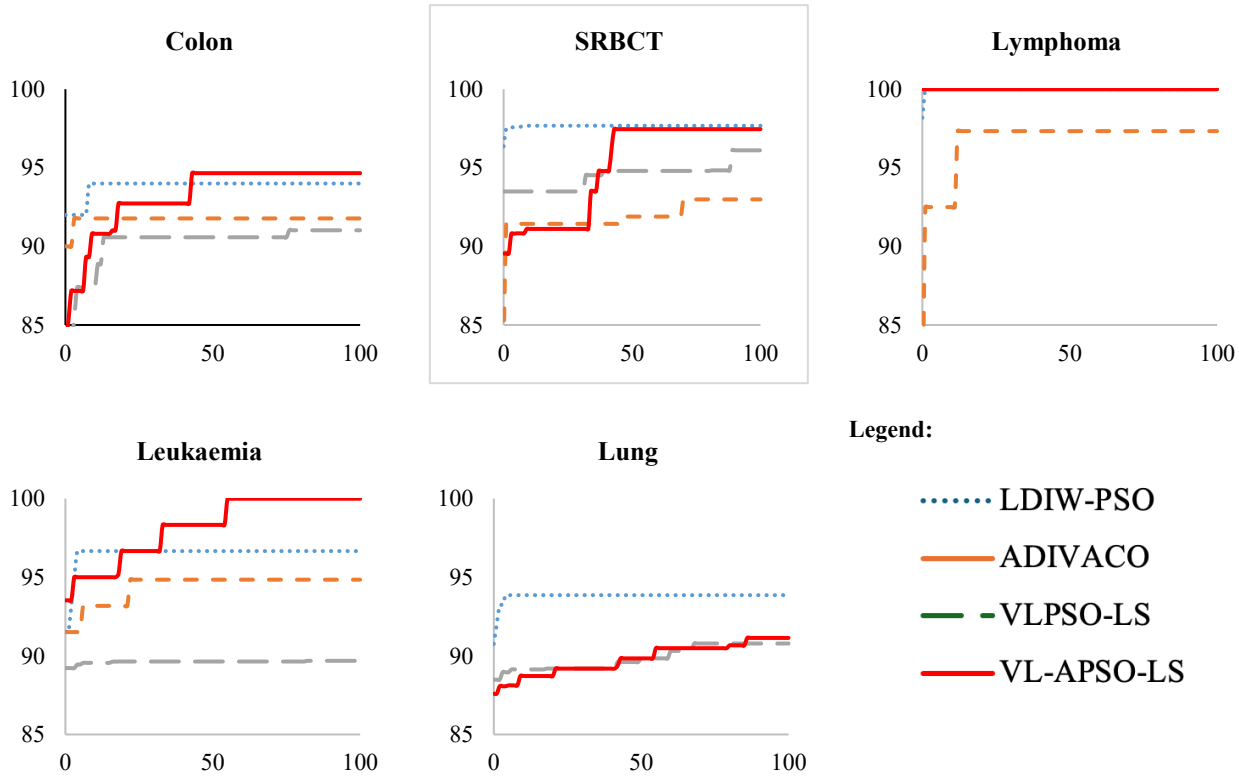


Fig. 7. Convergence behaviour analysis of VL-APSO-LS compared to state-of-the-art methods

As illustrated in Figure 7, across the Colon, SRBCT, Lymphoma, and Leukaemia datasets, VL-APSO-LS achieves higher fitness values in fewer iterations, indicating a superior exploration-exploitation balance. Although performance differences are less pronounced on the Lung dataset, VL-APSO-LS maintains competitive convergence stability, ranking second. Overall, the results confirm that integrating adaptive velocity learning and local search mechanisms enhances optimisation efficiency and improves fitness performance across diverse high-dimensional classification problems.

4.3.2. Comparative performance evaluation

As shown in Table **9**. VL-APSO-LS consistently demonstrates competitive or superior classification performance across most datasets. In terms of accuracy, the proposed method achieves the highest performance on the Colon, Leukaemia, and Lung datasets, while maintaining competitive results on the SRBCT and Lymphoma datasets. Notably, VL-APSO-LS achieves perfect classification accuracy (100%) in the Leukaemia dataset, highlighting its strong discriminative capability.

Tab. 9. Comparative performance of VL-APSO-LS and prior methods across five benchmark datasets

Dataset	Method	Time (s)	Size	Best Accuracy	Mean ± Std Accuracy	Wilcoxon S
Colon	LDIW-PSO	741.35	778.9	94		+
	ADIVACO	427.4	998.15	91.78		+
	VLPSO-LS	54	491	91.02		+
	VL-APSO-LS	56	86	94.66	85.85 ± 7.69	
SRBCT	LDIW-PSO	1056.3	1084.1	100		-
	ADIVACO	334.51	1155.4	100		-
	VLPSO-LS	128	571	100		+
	VL-APSO-LS	147	243	100	98.97 ± 3.17	
Lymphoma	LDIW-PSO	1523.79	1843.6	100		=
	ADIVACO	411.3	2013.3	100		=
	VLPSO-LS	490	486	100		=
	VL-APSO-LS	550	303	100	97.67 ± 6.80	
Leukaemia	LDIW-PSO	2411.418	3281.5	96.67		+
	ADIVACO	1192.517	3566.35	94.85		+
	VLPSO-LS	608	119	96.75		+
	VL-APSO-LS	773	850	100	95.88 ± 6.56	
Lung	LDIW-PSO	6131	5889.55	93.86		+
	ADIVACO	11110.7	6295.2	90.24		+
	VLPSO-LS	10916	2136	93.93		+
	VL-APSO-LS	11728	2202	95.62	94.14 ± 5.27	

Beyond accuracy, VL-APSO-LS demonstrates strong feature selection capability. For instance, in the Colon dataset, it selects only 86 features compared to 778.9 and 998.15 features selected by LDIW-PSO and ADIVACO, respectively. This substantial reduction underscores its effectiveness in identifying compact, informative gene subsets, which is critical for interpretability in biomedical applications. In terms of computational time, VL-APSO-LS is moderate. While it is not always the fastest method, its computational cost remains reasonable considering the significant improvements in accuracy and feature reduction. The increased computation time observed for the Leukaemia and Lung datasets is primarily due to their substantially higher dimensionality, which leads to considerably larger search spaces during optimisation. In these datasets, the adaptive velocity learning and local search mechanisms require additional fitness evaluations and feature subset refinements before convergence, thereby increasing computational complexity. This effect is particularly evident in the Lung dataset, which contains the largest number of genes among all evaluated datasets. Nevertheless, the additional computational effort is accompanied by improved classification performance and more compact feature subsets, indicating a practical trade-off between optimisation quality and execution time in extremely high-dimensional feature selection problems.

4.3.3. Statistical validation

The Wilcoxon signed-rank test further confirms the statistical superiority of VL-APSO-LS in most datasets, as indicated by the dominance symbols (+). The results suggest that the observed performance improvements are not due to random variation but are statistically significant. When equal performance (=) is observed, VL-APSO-LS remains competitive with existing methods. Overall, the results demonstrate that VL-APSO-LS achieves a favourable balance between classification accuracy, feature subset compactness, and computational efficiency. The consistent statistical superiority across multiple datasets validates the robustness and generalisation capability of the proposed approach for high-dimensional microarray classification problems.

Moreover, the stable convergence behaviour enhances reliability in real-world decision-support systems, where consistent optimisation outcomes are essential. The statistically validated superiority across heterogeneous datasets further confirms the robustness and generalisation capability of the proposed framework.

5. CONCLUSIONS

This study proposed an enhanced hybrid feature selection framework, VL-APSO-LS, which integrates adaptive velocity learning and local search mechanisms to improve the stability of optimisation and classification performance in high-dimensional gene expression datasets. Extensive experiments on five benchmark microarray datasets demonstrated that the proposed approach generally achieves competitive, and in many cases superior, classification accuracy compared with baseline and state-of-the-art PSO-based methods. However, the baseline approach remained competitive across several experimental settings, suggesting that the effectiveness of the proposed adaptive mechanisms may vary with dataset characteristics and classifier configurations. The results indicate that VL-APSO-LS effectively balances exploration and exploitation, as evidenced by its accelerated and stable convergence behaviour. Notable improvements were observed in the Colon, Lymphoma, and Leukaemia datasets, particularly when combined with SVM and NB classifiers. Moreover, the method demonstrated strong feature selection capability by substantially reducing redundant genes whilst maintaining or improving predictive performance. The Accuracy-to-Feature Ratio (AFR) analysis further confirmed the efficiency of the proposed adaptive schemes in balancing dimensionality reduction and classification accuracy.

Statistical validation through the Wilcoxon signed-rank test, alongside non-inferiority and superiority analyses, reinforced the robustness of the proposed method. Across most datasets and classifiers, VL-APSO-LS established either statistical superiority or non-inferiority relative to the baseline approach. These findings suggest that the observed performance improvements are generally robust and are unlikely to be attributable solely to random variation, although the magnitude of improvement varies across datasets and classifiers. Furthermore, the convergence analysis supports the stability of the optimisation process, reducing the risk of premature convergence in high-dimensional search spaces. From a practical perspective, the ability of VL-APSO-LS to generate compact yet discriminative gene subsets makes it particularly suitable for biomarker discovery and cancer classification tasks. Reduced feature dimensionality enhances interpretability and may lower downstream validation costs in clinical settings. Additionally, the competitive performance observed across multiple classifiers suggests that the framework exhibits a degree of classifier independence, thereby supporting its potential adaptability within real-world biomedical decision-support systems.

Despite these promising findings, several limitations should be acknowledged. First, the experiments were conducted on microarray datasets with relatively small sample sizes, which may limit generalisability to larger genomic datasets such as RNA-sequencing data. In addition, although the proposed framework demonstrated effective feature reduction and competitive classification performance, the biological relevance and stability of the selected gene subsets were not explicitly investigated in this study. Future work should evaluate feature selection stability across cross-validation folds and repeated runs, and examine the biological significance of frequently selected genes through pathway enrichment analysis and biomarker validation against external biological databases. Secondly, the current implementation relies on fixed classifier configurations; further investigation into joint hyperparameter optimisation may yield additional performance improvements. Although the present study focused on classification accuracy and optimisation-oriented performance measures, future work may incorporate additional evaluation metrics such as balanced accuracy, sensitivity, specificity, precision, recall, F1-score, MCC, and confusion matrix analysis to provide a more comprehensive assessment, particularly for larger, multi-class, or highly imbalanced genomic datasets.

In summary, VL-APSO-LS provides a statistically validated, robust, and efficient optimisation framework for high-dimensional genomic classification. The proposed adaptive strategy demonstrates the potential to improve predictive performance while contributing to feature compactness and convergence stability, positioning it as a promising approach for advanced bioinformatics and computational intelligence applications.

Funding

This project is supported by the Fundamental Research Grant Scheme (FRGS/1/2022/ICT02/UPSI/02/1) under the Ministry of Higher Education of Malaysia.

Authorship contribution

Conceptualisation, Siti Ramadhani and Shir Li Wang; methodology, Siti Ramadhani; software, Siti Ramadhani and Haldi Budiman; validation, Muhammad Fikry and Roziana Ariffin and Shir Li Wang; formal analysis, Siti Ramadhani; investigation, Siti Ramadhani; writing-original draft preparation, Siti Ramadhani; writing-review and editing, Haldi Budiman and Theam Foo Ng and Sumayyah Dzulkifly and Shir Li Wang; supervision, Haldi Budiman and Shir Li Wang; project administration, Sumayyah Dzulkifly and Shir Li Wang; funding acquisition, Shir Li Wang. All authors reviewed the results and approved the final version of the manuscript.

Conflicts of Interest

The authors declare no conflicts of interest to report regarding the present study.

REFERENCES

Ajibade, S., Ajibade, S.-S. M., Areche, F. O., Dante, D., Flores, C., & Mavel, G. (2023). An insight into the modification of inertia weight of PSO for feature selection. *Biomechanical Science and Engineering*, *1*(1), 683–700. https://doi.org/10.17605/OSF.IO/R2ZUF

Algamal, Z. Y., Alhamzawi, R., & Mohammad Ali, H. T. (2018). Gene selection for microarray gene expression classification using Bayesian Lasso quantile regression. *Computers in Biology and Medicine*, *97*, 145–152. https://doi.org/10.1016/j.compbiomed.2018.04.018

Alomari, O. A., Khader, A. T., Betar, M. A., & Awadalllah, M. A. (2020). A novel gene selection method using modified MRMR and hybrid Bat Inspired with Hill Climbing Algorithm. *Applied Intelligence*, *48*(1), 4429–4447.

Ampomah, E. K., Qin, Z., & Nyame, G. (2020). Evaluation of tree-based ensemble machine learning models in predicting stock price direction of movement. *Information*, *11*(6), Article 332. https://doi.org/10.3390/info11060332

Azar, A. T., Khan, Z. I., Amin, S. U., & Fouad, K. M. (2023). Hybrid global optimization algorithm for feature selection. *Computers, Materials and Continua*, *74*(1), 2021–2037. https://doi.org/10.32604/cmc.2023.032183

Bi, J., Wang, Z., Yuan, H., Zhang, J., & Zhou, M. C. (2023). Self-adaptive teaching-learning-based optimizer with improved RBF and sparse autoencoder for high-dimensional problems. *Information Sciences*, *630*, 463–481. https://doi.org/10.1016/j.ins.2023.02.044

Bokhare, A., & Jha, P. (2023). Machine learning models applied in analyzing breast cancer classification accuracy. *IAES International Journal of Artificial Intelligence*, *12*(3), 1370–1377. https://doi.org/10.11591/ijai.v12.i3.pp1370-1377

Camalan, S., Mahmood, H., Binol, H., Araújo, A. L. D., Santos-Silva, A. R., Vargas, P. A., Lopes, M. A., Khurram, S. A., & Gurcan, M. N. (2021). Convolutional neural network-based clinical predictors of oral dysplasia: Class activation map analysis of deep learning results. *Cancers*, *13*(6), Article 1291. https://doi.org/10.3390/cancers13061291

Cao, D., Xu, Y., Yang, Z., Dong, H., & Li, X. (2023). An enhanced whale optimization algorithm with improved dynamic opposite learning and adaptive inertia weight strategy. *Complex & Intelligent Systems*, *9*(1), 767–795. https://doi.org/10.1007/s40747-022-00827-1

Gad, A. G. (2022). Particle swarm optimization algorithm and its applications: A systematic review. *Archives of Computational Methods in Engineering*, *29*(5), 2531–2561. https://doi.org/10.1007/s11831-021-09694-4

Gibbons, J. D., & Chakraborti, S. (2003). *Nonparametric statistical inference* (4th ed.). Marcel Dekker.

Hamed, T., Dara, R., & Kremer, S. C. (2018). Network intrusion detection system based on recursive feature addition and bigram technique. *Computers & Security*, *73*, 137–155. https://doi.org/10.1016/j.cose.2017.10.011

Jain, M., Saihjpal, V., Singh, N., & Singh, S. B. (2022). An overview of variants and advancements of PSO algorithm. *Applied Sciences*, *12*(17), Article 8392. https://doi.org/10.3390/app12178392

Ji, B., Lu, X., Sun, G., Zhang, W., Li, J., & Xiao, Y. (2020). Bio-inspired feature selection: An improved binary particle swarm optimization approach. *IEEE Access*, *8*, 85989–86002. https://doi.org/10.1109/ACCESS.2020.2992752

Kennedy, J. (1997). Particle swarm: Social adaptation of knowledge. In *Proceedings of the 1997 IEEE International Conference on Evolutionary Computation (ICEC)* (pp. 303–308). IEEE. https://doi.org/10.1109/ICEC.1997.592326

Kennedy, J., & Eberhart, R. C. (1997). Discrete binary version of the particle swarm algorithm. In *Proceedings of the 1997 IEEE International Conference on Systems, Man, and Cybernetics* (Vol. 5, pp. 4104–4108). IEEE. https://doi.org/10.1109/ICSMC.1997.637339

Li, J., Cheng, K., Wang, S., Morstatter, F., Trevino, R. P., Tang, J., & Liu, H. (2018). Feature selection: A data perspective. *ACM Computing Surveys*, *50*(6), 1–45. https://doi.org/10.1145/3136625

Li, M., Chen, H., Shi, X., Liu, S., Zhang, M., & Lu, S. (2019). A multi-information fusion "triple variables with iteration" inertia weight PSO algorithm and its application. *Applied Soft Computing*, *84*, Article 105677. https://doi.org/10.1016/j.asoc.2019.105677

Mahesh, T. R., Kumar, V. V., Kumar, V. D., Geman, O., Margala, M., & Guduri, M. (2023). The stratified K-folds cross-validation and class-balancing methods with high-performance ensemble classifiers for breast cancer classification. *Healthcare Analytics*, *4*, Article 100247. https://doi.org/10.1016/j.health.2023.100247

Mohamed, M., Abdullah, A., Zaki, A. M., Rizk, F. H., Eid, M. M., & El-Kenaway, E. M. (2024). Advances and challenges in feature selection methods: A comprehensive review. *Journal of Artificial Intelligence and Metaheuristics*, *7*(1), 67–77. https://doi.org/10.54216/JAIM.070105

Mohammed, N. S., & Beitollahi, H. (2022). Accurate classification in uncertainty dataset using particle swarm optimization-trained radial basis function. *Journal of Intelligent & Fuzzy Systems*, *43*(2), 1660–1672. https://doi.org/10.3233/JIFS-213120

Nouri-Moghaddam, B. (2023). A novel bio-inspired hybrid multi-filter wrapper gene selection method with ensemble classifier for microarray data. *Neural Computing and Applications*, *35*(16), 11531–11561. https://doi.org/10.1007/s00521-023-08312-3

Ozcan, I., Aydin, H., & Cetinkaya, A. (2022). Comparison of classification success rates of different machine learning algorithms in the diagnosis of breast cancer. *Asian Pacific Journal of Cancer Prevention*, *23*(10), 3287–3297. https://doi.org/10.31557/APJCP.2022.23.10.3287

Papazoglou, G., & Biskas, P. (2023). Review and comparison of genetic algorithm and particle swarm optimization in the optimal power flow problem. *Energies*, *16*(3), Article 1152. https://doi.org/10.3390/en16031152

Peng, C., Wu, X., Yuan, W., Zhang, X., Zhang, Y., & Li, Y. (2021). MGRFE: Multilayer recursive feature elimination based on an embedded genetic algorithm for cancer classification. *IEEE/ACM Transactions on Computational Biology and Bioinformatics*, *18*(2), 621–632. https://doi.org/10.1109/TCBB.2019.2921961

Ravenzwaaij, D. V., Monden, R., Tendeiro, J. N., & Ioannidis, J. P. A. (2019). Bayes factors for superiority, non-inferiority, and equivalence designs. *BMC Medical Research Methodology*, *19*(1), Article 71. https://doi.org/10.1186/s12874-019-0699-7

Saraf, T. O. Q., Fuad, N., & Taujuddin, N. S. A. M. (2023). Framework of meta-heuristic variable length searching for feature selection in high-dimensional data. *Computers*, *12*(1), Article 7. https://doi.org/10.3390/computers12010007

Shami, T. M., Al-Tashi, Q., Khodadadi, N., Abdulkadir, S. J., Ahmed, A., & Mirjalili, S. (2025). Dimension selection: An innovative metaheuristic strategy for particle swarm optimization. *Cluster Computing*, *28*(1), Article 379. https://doi.org/10.1007/s10586-025-05201-7

Shami, T. M., El-Saleh, A. A., Alswaitti, M., Al-Tashi, Q., Summakieh, M. A., & Mirjalili, S. (2022). Particle swarm optimization: A comprehensive survey. *IEEE Access*, *10*, 10031–10061. https://doi.org/10.1109/ACCESS.2022.3142859

Stefanos, R., D'Arrigo, G., & Tripepi, G. (2020). Methodological aspects of superiority, equivalence, and non-inferiority trials. *Internal and Emergency Medicine*, *15*(6), 1085–1091. https://doi.org/10.1007/s11739-020-02450-9

Tran, B., Xue, B., & Zhang, M. (2019). Variable-length particle swarm optimization for feature selection on high-dimensional classification. *IEEE Transactions on Evolutionary Computation*, *23*(3), 473–487. https://doi.org/10.1109/TEVC.2018.2869405

Tran, B., Xue, B., Zhang, M., & Nguyen, S. (2016). Investigation on particle swarm optimisation for feature selection on high-dimensional data: Local search and selection bias. *Connection Science*, *28*(3), 270–294. https://doi.org/10.1080/09540091.2016.1185392

Trelea, I. C. (2003). The particle swarm optimization algorithm: Convergence analysis and parameter selection. *Information Processing Letters*, *85*(6), 317–325. https://doi.org/10.1016/S0020-0190(02)00447-7

Wasserstein, R. L., & Lazar, N. A. (2016). The ASA's statement on p-values: Context, process, and purpose. *The American Statistician*, *70*(2), 129–133. https://doi.org/10.1080/00031305.2016.1154108

Xue, B., Zhang, M., & Browne, W. N. (2013). Particle swarm optimization for feature selection in classification: A multi-objective approach. *IEEE Transactions on Cybernetics*, *43*(6), 1656–1671. https://doi.org/10.1109/TSMCB.2012.2227469

Zhang, J., & Sanderson, A. C. (2007). JADE: Self-adaptive Differential Evolution with fast and reliable convergence performance. In *2007 IEEE Congress on Evolutionary Computation (CEC 2007)* (pp. 2251–2258). IEEE. https://doi.org/10.1109/CEC.2007.4424751

Zhang, X.-Y., Liu, C.-L., & Suen, C. Y. (2020). Towards robust pattern recognition: A review. *IEEE Transactions on Pattern Analysis and Machine Intelligence*, *42*(6), 1320–1336. https://doi.org/10.1109/TPAMI.2019.2893220

Zhu, Z., Ong, Y.-S., & Dash, M. (2007). Markov blanket-embedded genetic algorithm for gene selection. *Pattern Recognition*, *40*(11), 3236–3248. https://doi.org/10.1016/j.patcog.2007.02.007